

# Evidence for the Importance of Atmospheric Nitrogen Deposition to Eutrophic Lake Dianchi, China

Xiaoying Zhan,<sup>▲,†</sup> Yan Bo,<sup>▲,†</sup> Feng Zhou,<sup>\*,†,Ⓜ</sup> Xuejun Liu,<sup>‡</sup> Hans W. Paerl,<sup>§,◆</sup> Jianlin Shen,<sup>||</sup> Rong Wang,<sup>⊥</sup> Farong Li,<sup>#</sup> Shu Tao,<sup>†,Ⓜ</sup> Yanjun Dong,<sup>○</sup> and Xiaoyan Tang<sup>▽</sup>

<sup>†</sup>Sino-France Institute of Earth Systems Science, Laboratory for Earth Surface Processes, College of Urban and Environmental Sciences, Peking University, Beijing 100871, P.R. China

<sup>‡</sup>College of Resources and Environmental Sciences, China Agricultural University, Beijing 100193, P.R. China

<sup>§</sup>Institute of Marine Sciences, University of North Carolina at Chapel Hill, Morehead City, North Carolina 28557, United States

<sup>||</sup>Key Laboratory of Agro-Ecological Processes in Subtropical Regions, Institute of Subtropical Agriculture, Chinese Academy of Sciences, Changsha, Hunan 410125, P.R. China

<sup>⊥</sup>Department of Global Ecology, Carnegie Institution for Science, Stanford, California 94305, United States

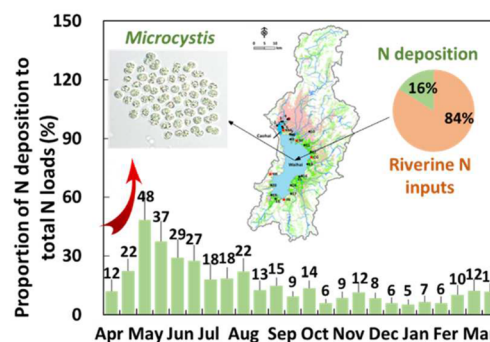
<sup>#</sup>Kunming Environmental Monitoring Center, Kunming, Yunnan 650028, P.R. China

<sup>▽</sup>College of Environmental Sciences and Engineering, Peking University, Beijing 100871, P.R. China

<sup>○</sup>Laboratory of the Pear River Estuarine Dynamics and Associated Process Regulation, Pearl River Hydraulic Research Institute, Guangzhou 510611, P.R. China

<sup>◆</sup>College of Environment, Hohai University, Nanjing 210098, P.R. China

**ABSTRACT:** Elevated atmospheric nitrogen (N) deposition has significantly influenced aquatic ecosystems, especially with regard to their N budgets and phytoplankton growth potentials. Compared to a considerable number of studies on oligotrophic lakes and oceanic waters, little evidence for the importance of N deposition has been generated for eutrophic lakes, even though emphasis has been placed on reducing external N inputs to control eutrophication in these lakes. Our high-resolution observations of atmospheric depositions and riverine inputs of biologically reactive N species into eutrophic Lake Dianchi (the sixth largest freshwater lake in China) shed new light onto the contribution of N deposition to total N loads. Annual N deposition accounted for 15.7% to 16.6% of total N loads under variable precipitation conditions, 2-fold higher than previous estimates (7.6%) for the Lake Dianchi. The proportion of N deposition to total N loads further increased to 27–48% in May and June when toxic blooms of the ubiquitous non-N<sub>2</sub> fixing cyanobacteria *Microcystis* spp. are initiated and proliferate. Our observations reveal that reduced N (59%) contributes a greater amount than oxidized N to total N deposition, reaching 56–83% from late spring to summer. Progress toward mitigating eutrophication in Lake Dianchi and other bloom-impacted eutrophic lakes will be difficult without reductions in ammonia emissions and subsequent N deposition.



## INTRODUCTION

Human activities have significantly increased emissions of reactive nitrogen (N, including reduced and oxidized forms) to the atmosphere and their resultant deposition.<sup>1,2</sup> Results of global atmospheric chemical transport models indicated that atmospheric deposition of N has increased by approximately 3-fold since preindustrial times, especially over the East and South Asia.<sup>3</sup> The ecological effects of elevated atmospheric N deposition have been observed or modeled for oligotrophic lakes and oceanic waters, showing that such N inputs can stimulate phytoplankton growth.<sup>4–7</sup> This also leads to an increase in the stoichiometric N/phosphorus (P) ratio, which can induce a shift from N-limited to P-limited phytoplankton.<sup>3,4</sup> In contrast, the contribution made by atmospherically deposited

N to the total N input for eutrophic lakes has rarely received attention,<sup>8,9</sup> because it was commonly considered to be much less than N inputs from watersheds to these lakes.<sup>10</sup>

However, recent evidence from the few field observations demonstrated that the contribution of N deposition cannot be neglected compared to riverine inputs for eutrophic lakes. For instance, Luo et al.<sup>9</sup> measured wet N deposition in mesotrophic Lake Taihu, the third largest freshwater lake in China, indicating that atmospheric inputs of N accounted for approximately 14%

Received: December 5, 2016

Revised: June 1, 2017

Accepted: June 1, 2017

Published: June 1, 2017

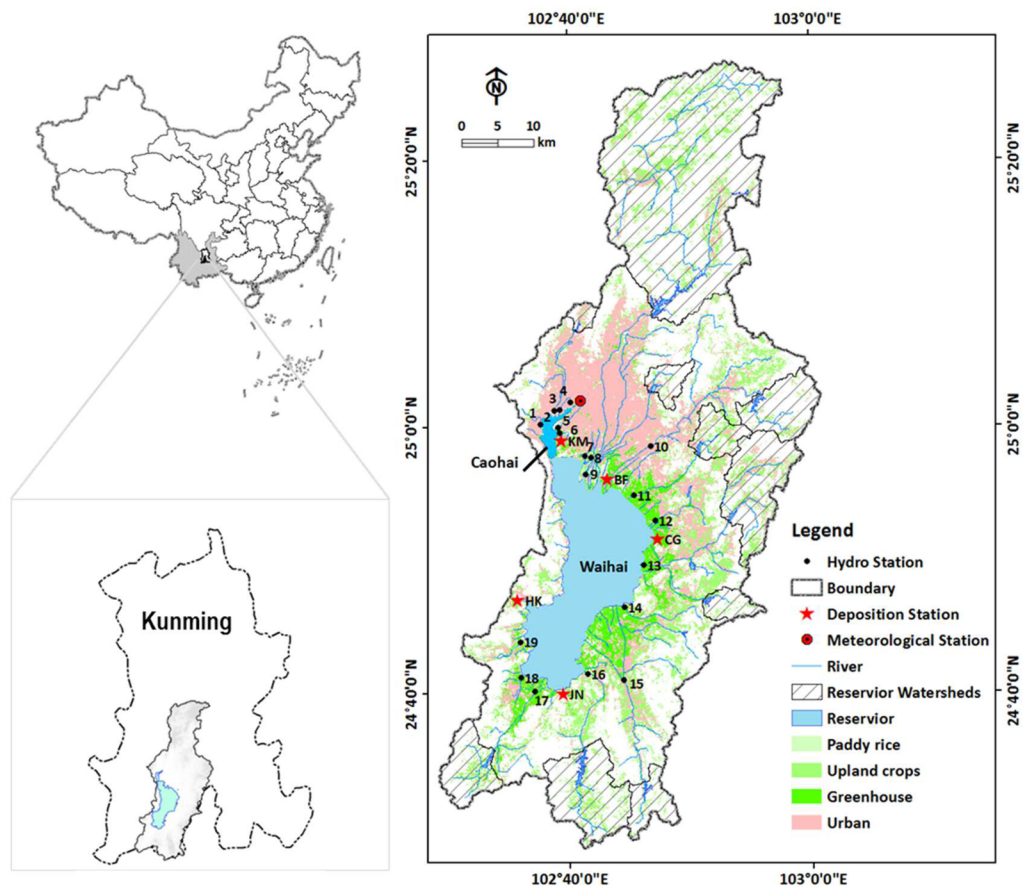


**Figure 1.** Locations of Lake Dianchi watershed and sampling sites. Nineteen rivers, accounting for 95% of lake's inflow, were chosen for measuring N concentration and discharge. The rivers numbered 1 to 6 flowed into Caohai, while the rest flowed into Waihai. Hatch marks indicate the area controlled by 10 large to medium-size reservoirs.

of total N inputs. A similar percentage was reported for a mesotrophic lake in Venezuela<sup>11</sup> (Lake Maracaibo, wet deposition, 19%). Furthermore, the percentage increased considerably when both dry and wet deposition (i.e., gaseous, particulate and dissolved N) were included.<sup>12</sup> With long-term controls of point and nonpoint sources from watersheds taking place in developed countries, atmospheric N deposition is becoming an increasingly dominant N source to these waters (e.g., 15–42% of the total N inputs<sup>13</sup> in the northeastern and mid-Atlantic regions of the United States).

However, the contribution made by atmospheric N deposition to total inputs remains challenging to accurately assess, especially at a high-resolution temporal scale. Multiple factors are associated with the difficulty in assessment, especially when quantifying dry deposition and N inputs from watersheds to receiving waters. First, gaseous N (i.e., ammonia [NH<sub>3</sub>], nitrogen dioxide [NO<sub>2</sub>], nitric acid and nitrous acid [HNO<sub>2</sub>/HNO<sub>3</sub>]) deposition have generally been ignored or are only partially considered by current observation networks globally (e.g., EANET,<sup>14</sup> CASTNET,<sup>15</sup> AMoN,<sup>15</sup> IMPROVE NH<sub>x</sub>,<sup>15</sup> and EMEP<sup>16</sup>) and in previous regional assessments.<sup>12</sup> Likewise, wet or bulk deposition of inorganic N (NH<sub>4</sub><sup>+</sup>-N + NO<sub>3</sub><sup>-</sup>-N) has been measured systematically in China, but organic N was seldom analyzed.<sup>12</sup> Those omissions may result in a considerable underestimation of direct atmospheric N deposition to these waters. Second, most measurements applying passive samplers yield ambient exposures on a monthly interval, mainly due to low

concentrations of gaseous or particulate N.<sup>12</sup> Although active samplers (e.g., denuder systems) can be deployed to determine hourly or daily concentrations of gaseous constituents and fine-fraction particulates,<sup>17</sup> they are unsuitable for long-term field observations without a power supply.<sup>12</sup> In addition, riverine N inputs (i.e., N concentration × river discharge) were generally determined by using process-based models that simulate the N available for transport to the waters from different watershed N sources (runoff from agriculture, urban areas and upland forests, point sources).<sup>13,18,19</sup> A key limitation in such models is the large uncertainties arising from model structure and parameter choices.<sup>20</sup> Such uncertainties can be reduced by performing observations of river discharge and N concentrations at high spatial and temporal resolutions.

The primary objective of this study is to test the hypothesis that atmospheric N deposition makes an important contribution to total N loads for eutrophic Lake Dianchi, the sixth largest freshwater lake in China, through high-resolution (daily or biweekly) systematic observations of N deposition and inputs. Dry and wet deposition fluxes of all N species and riverine N inputs were quantified and their annual and biweekly contributions to total N loads were determined. In addition, we considered the reliability of the fluxes as well as the importance of N deposition on lake eutrophication, and implications for lake ecosystem management.

## MATERIALS AND METHODS

**Study Area.** Lake Dianchi is located in Southwest China (24°29′ to 25°28′N, 102°29′ to 103°01′E). It has a surface area of 310 km<sup>2</sup> at the elevation of 1887.5 m, a mean depth of 5.3 m, a shoreline of 150 km, and water retention time of 3.5 years<sup>21</sup> (Figure 1). Watershed area for Lake Dianchi is 2920 km<sup>2</sup>, of which 1088.6 km<sup>2</sup> is controlled by 10 large to medium-size reservoirs that have no outflows (Figure 1). The lake is artificially divided into two segments by an embankment and a dam, where the area of the northern part (Caohai) is ~12 km<sup>2</sup> surrounded by urban area of Kunming city and the southern part (Waihai, 298 km<sup>2</sup>) is bordered by an intensively managed farmland. Land use in the watershed is primarily forest (47%), cropland (20%), and urban areas (16%; Figure 1). The total population in the Lake Dianchi Watershed has increased steadily from 1.8 million in 1992 to 4.1 million in 2015. Consequently, the lake has suffered from severe eutrophication, despite the fact that approximately 52 billion RMB (equal to 7.7 billion in USD) has been invested to mitigate lake eutrophication by the Chinese Central Government during 1996–2015.<sup>22</sup>

**Dry N Deposition Samples around the Lake.** Sampling of dry N deposition, including gaseous and particulate N, was conducted from April 1, 2010 to March 31, 2011. Five deposition monitoring stations were evenly located around Lake Dianchi (Figure 1), including Kunming (KM), Baofeng (BF), Chenggong (CG), Jinning (JN), and Haikou (HK). For each station, Ogawa passive samplers (Ogawa & Co., FL, U.S.A.) were used to collect ammonia [NH<sub>3</sub>] and nitrogen dioxide [NO<sub>2</sub>] samples, which showed no significant differences from the continuous active samplers used in previous studies.<sup>23</sup> Another passive sampler (USDA Forest Service, CA, U.S.A.) was used for collecting nitrous acid/nitric acid [HNO<sub>2</sub>/HNO<sub>3</sub>] samples. Previous comparative experiments showed that this sampler was reliable for determining wide ranges of ambient HNO<sub>2</sub>/HNO<sub>3</sub>.<sup>24</sup> Detailed descriptions of these passive samplers can be found in Roadman et al.<sup>25</sup> and Bytnerowicz et al.<sup>26</sup> High volume aerosol samplers (Laoshan Elec. Inc., Qingdao, China) were applied to collect total suspended particulates (TSP) at a flow rate of 1.05 m<sup>3</sup> min<sup>-1</sup>. Three replicate samplers for dry N deposition were installed at a height of 3.5 m from the ground and at a distance of <50 m from the shoreline of Lake Dianchi. Passive samplers for gaseous N were exposed for 2 weeks, while active samplers for particulate N were operated 24 h every week on Monday, but was manually halted during rainfall events. The exposed samplers were placed in a resealable plastic bag, the bagged sampler was placed into a brown airtight container taken to laboratory for analysis. Detailed information for collection and measurements are provided in Text S1 of the Supporting Information (SI).

**Wet N Deposition Samples around the Lake.** At five deposition monitoring stations, rainfall samples were taken on an event basis using a stainless steel funnel and plexiglass bottle, along with precipitation automatically measured by tipping-bucket rain gauge (Guoxinhuayuan Tech. Inc., Beijing, China). The collector was kept completely closed and was opened only at the beginning of a rainfall event by the staff from the Kunming Environmental Monitoring Center (KEMC). The collected samples were then immediately stored in acid-washed high density polyethylene (HDPE) bottles. To prevent biological utilization of deposited N, chloroform was used as a biocide in the wet bottle. A cap covered the “wet” bottle which, in combination with the inherently low rainwater pH of 4 to 5, minimized the potential for NH<sub>3</sub> volatilization. Wet deposition

was sampled for all rainfall events having precipitation of >2 mm. All collected samples were frozen at -18 °C at each site until delivery to the laboratory for analysis. Collectors were cleaned for each event with 1% HCl and Nanopure water.

**River Discharge and Water Samples.** Although river discharges data were not available except for Panlongjiang (No. 8) and Baoxiang (No. 10) Rivers, water levels in the other 17 rivers were continuously measured in this study (Figure 1). These 19 rivers contribute more than 95% of lake’s streamflow.<sup>27</sup> The rating curves were developed by simultaneously measuring water levels and the current velocities for a cross-section of each river following the USGS guideline for the current-meter method,<sup>28</sup> where the sizes of cross-section (i.e., width, depth, and area) were measured for each river (Table S1). To ensure rating curves over a wide range of flow rates, enhanced observations were conducted for three stormwater events (precipitation >30 mm day<sup>-1</sup>). Each sampling procedure lasted more than 48 h per event. The 10-min water levels were continuously observed for each tributary by HOBO data logger (U20-001-01, Onset Computer Corporation, MA, U.S.A.), and the current velocities were measured by the Global Water flow probe (FP201) in each subsection of a channel cross-section. Water level was further converted into daily discharge based on the derived rating curves for each river. In addition, vertical water samplers were used to collect water samples of 19 rivers on biweekly interval. The procedure was referenced to the Technical Specifications Requirements for Monitoring of Surface Water and Waste Water in China (HJ/T91–2002). As all rivers have width of ≤50 m and depth of ≤5 m (Table S1), one sample was collected in the river centerline at 0.5 m below or half depth of the river. All water samples were rapidly transported to the KEMC for analysis.

**Chemical Analysis.** After the exposures, all filters for gaseous and particulate N were placed in polyethylene tubes into which 8 and 20 mL distilled/deionized water was added, respectively. The tubes were shaken on a shaker for 15 min at midrange speed. The extracted solutions of dry deposition, wet deposition samples, and water samples were then filtered with a 0.45 μm syringe filter. N quantities in the filtered solutions were analyzed following the Standard Methods for the Examination of Water and Wastewater<sup>29</sup> in China. Ammonium nitrogen [NH<sub>4</sub><sup>+</sup>-N], nitrate nitrogen [NO<sub>3</sub><sup>-</sup>-N], total nitrogen (TN), and Kjeldahl nitrogen (KTN) were measured by Nessler’s reagent colorimetric method, ultraviolet spectrophotometric method, K<sub>2</sub>S<sub>2</sub>O<sub>8</sub> oxidation-ultraviolet spectrophotometric method, as well as Semi-Micro-Kjeldahl method, respectively. Organic N was determined by the difference between KTN and NH<sub>4</sub><sup>+</sup>-N. The detection limits for NH<sub>4</sub><sup>+</sup>-N, NO<sub>3</sub><sup>-</sup>-N, TN, and KTN are 0.025, 0.02, 0.05, and 0.025 mg N L<sup>-1</sup>, respectively. For gaseous N deposition, ambient concentrations of NH<sub>3</sub>, NO<sub>2</sub>, and HNO<sub>2</sub>/HNO<sub>3</sub> were calculated as product of their quantities collected in passive samplers and conversion coefficients divided by exposure time (see details at <http://ogawausa.com/wp-content/uploads/2014/04/ConcentrationInAmbientAir.pdf> Concentration-InAmbientAir.pdf and Bytnerowicz et al.<sup>26</sup>). Additionally, for each batch of field exposed samples for gaseous and particulate N, three blank filters were also prepared to represent extracts from unexposed samplers that are prepared in the laboratory and transported between laboratory and monitoring sites. The blank samples were extracted and analyzed using the same methods as the exposed samples. The details of blank samples can be found in Text S1.

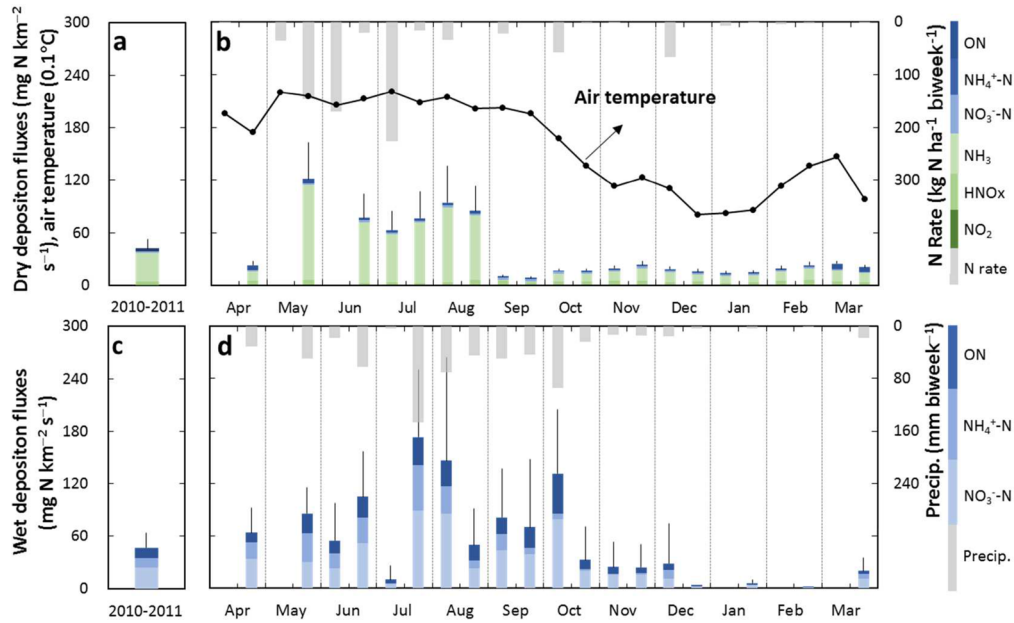


**Figure 2.** Temporal variation of atmospheric deposition of N species in 2010–2011. (a) Annual mean deposition fluxes of gaseous and particulate N and (b) on biweekly interval; (c) annual mean fluxes of wet deposition; and (d) on biweekly interval. Note: biweekly data sets of air temperature (black dot line) and precipitation (gray bar) at Kunming meteorological station are available online at <http://data.cma.cn/>; a time-series data set of fertilizer application rate (N rate; gray bar) was compiled through in-house surveys of 300 farmers surrounding Lake Dianchi; all error bars for simulated flux are one SD.

### Estimation of Deposition Fluxes and Riverine Inputs.

Biweekly flux of dry deposition ( $\text{mg km}^{-2} \text{s}^{-1}$ ) was calculated as a product of N concentration and deposition velocity ( $V_d$ ,  $\text{m s}^{-1}$ ) at each site. The concentrations of gaseous and particulate N were determined as described above.  $V_d$  of gaseous N and particulate N over lake surface was estimated by a well-tested deposition velocity model<sup>30</sup> combined with the on-site hourly meteorological data. One of the national meteorological stations was located at the north end of Lake Dianchi (Figure 1), where meteorological variables used in the model included air temperature, relative humidity, air pressure, solar radiation, wind speed at 10-m height ( $v_{10}$ ), precipitation, and dew point on hourly intervals. Prior to the estimate,  $v_{10}$  was converted into wind speed at 3.5-m height,  $v_{3.5}$ , according to a power law (i.e.,  $v_{3.5} = v_{10} \times (3.5/10)^\alpha$ , where  $\alpha$  was set as 0.1).<sup>31</sup> Gas  $V_d$  over Lake Dianchi was calculated using the big-leaf resistance analogy model.<sup>32</sup> In contrast to vegetation, roughness length was set as 0.0003 m based on the results for the East China Sea,<sup>33</sup> and surface resistance was set as  $0 \text{ s m}^{-1}$  for  $\text{NH}_3$  and  $\text{HNO}_3$  but  $20\,000 \text{ s m}^{-1}$  for  $\text{NO}_2$ .<sup>34</sup> Particulate  $V_d$  was parametrized according to Slinn,<sup>35</sup> where parameters related to surface resistance and gravitational settling velocity were determined according to Zhang et al.<sup>36</sup> Details of these models were described in Text S2. In addition, the flux of wet deposition was calculated as a product of N concentration and rainfall amount for each rainfall event and monitoring site.

Daily riverine N inputs were calculated as a function of river discharge, by means of Load Estimator (LOADEST):<sup>37</sup>

$$\ln(L_i) = a_0 + a_1 \ln Q + a_2 \ln Q^2 + a_3 \sin(2\pi d\text{time}) + a_4 \cos(2\pi d\text{time}) + a_5 d\text{time} + a_6 d\text{time}^2 + \varepsilon \quad (1)$$

where  $Q$  is daily river discharge,  $d\text{time}$  is decimal time,  $a_0 \sim a_6$  are the fitted coefficients in the multiple regression model, and  $\varepsilon$  is estimate error. Note that the biweekly TN concentration was

multiplied by the corresponding daily discharge so that eq 1 is a function of load ( $L_i$ ) instead of concentration. Within LOADEST, the model to estimate N loads was set to be automatically selected from predefined regression models.<sup>37</sup> To select the best one, LOADEST calculated model coefficients using each calibration data set (i.e., observed TN loads in few of days), and models with the lowest Akaike information criterion (AIC) values were selected for load estimations.

## RESULTS

**Dry N Deposition.** The N flux of dry deposition over the Lake Dianchi was  $42.1 \pm 10.3 \text{ mg km}^{-2} \text{ s}^{-1}$  in 2010–2011 ( $1\sigma$  as the standard deviation of fluxes occurring in 5 sites; Figure 2), with  $37.1 \pm 10.5 \text{ mg km}^{-2} \text{ s}^{-1}$  for gaseous N and  $5.0 \pm 0.7 \text{ mg km}^{-2} \text{ s}^{-1}$  for particulate N. The major species, accounting for 99% of the dry deposition, was  $\text{NH}_3$  ( $32.8 \pm 10.1 \text{ mg km}^{-2} \text{ s}^{-1}$ , 77.9%),  $\text{HNO}_2/\text{HNO}_3$  ( $4.0 \pm 0.6 \text{ mg km}^{-2} \text{ s}^{-1}$ , 9.5%), particulate ON ( $2.9 \pm 0.6 \text{ mg km}^{-2} \text{ s}^{-1}$ , 6.8%), and particulate  $\text{NO}_3^- \text{-N}$  ( $2.0 \pm 0.1 \text{ mg km}^{-2} \text{ s}^{-1}$ , 4.7%), while the rest of 1% were  $\text{NO}_2$  (0.7%) and particulate  $\text{NH}_4^+ \text{-N}$  (0.3%). The corresponding concentrations and  $V_d$  of gases and TSP at 5 sites can be found in Figures S1 and S2. Regardless of three missing samples in early April–June, the dry deposition N flux showed strong seasonality (Figure 2b). High fluxes were observed from May to August, which were 1.7–13.3 times higher than the remaining periods. Dry deposition of  $\text{NH}_3$  was the major source (>86.0%) of total dry deposition N flux from May to August, with biweekly coefficient of variation [CV] of 115%. The  $\text{NO}_2$  flux was highest in autumn and early winter ( $0.4 \pm 0.2 \text{ mg km}^{-2} \text{ s}^{-1}$ ) and remained low in early spring and summer ( $0.2 \pm 0.1 \text{ mg km}^{-2} \text{ s}^{-1}$ ). The remaining N fluxes were negligible with a seasonal variability with CV of ~27%.

**Wet N Deposition.** Wet deposition over the Lake Dianchi yielded an N flux of  $46.5 \pm 13.2 \text{ mg km}^{-2} \text{ s}^{-1}$ , 10.5% higher than dry deposition (Figure 2c).  $\text{NO}_3^- \text{-N}$  dominated the total flux of

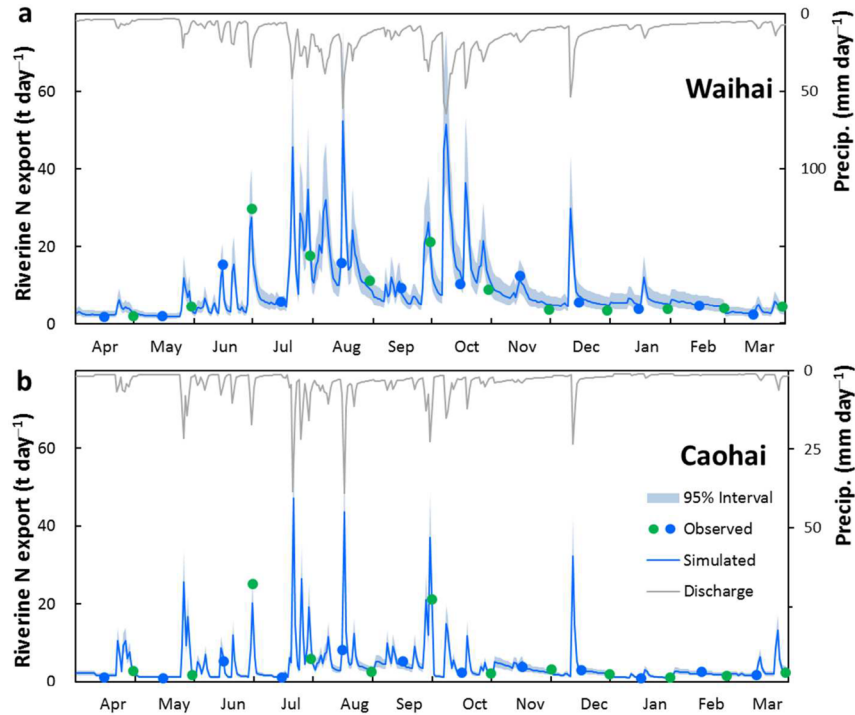


**Figure 3.** Total N inputs from watersheds to Lake Dianchi. (a) Waihai and (b) Caohai. Note: daily precipitation was observed in 5 deposition monitoring sites, as shown as gray line; the full data set of N inputs observed in the 15<sup>th</sup> day of the month is illustrated as blue solid circles, whereas the data from the routine monitoring program of Kunming City is represented as green solid circles. The N input estimations and uncertainties are shown as a mean value (curve) and 95% confidence interval (shaded area) derived from the LOADEST.

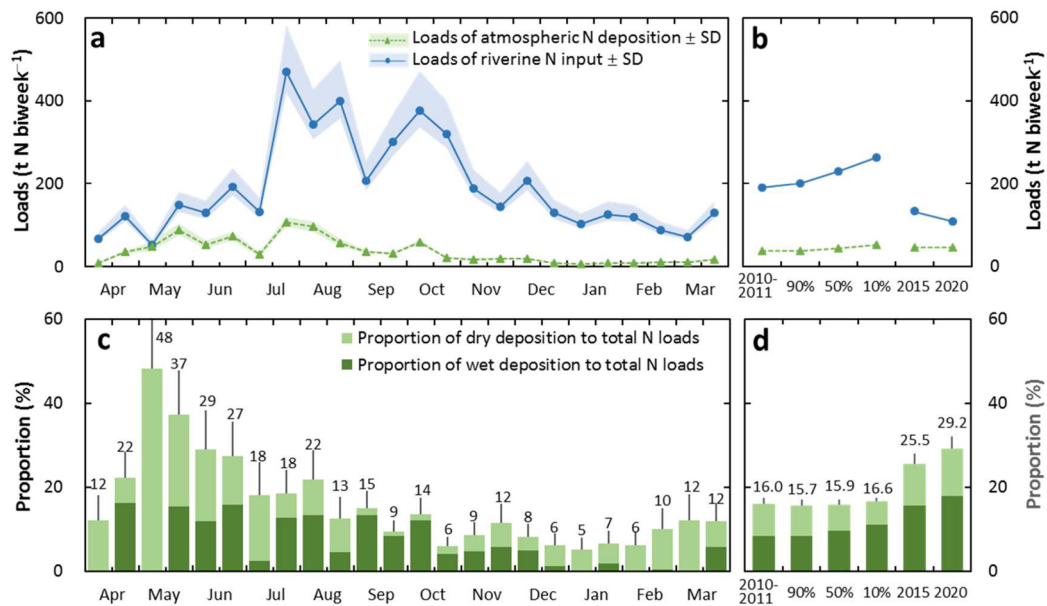


**Figure 4.** Proportion of atmospheric N deposition to total N loads. (a) Temporal variation of N deposition and inputs in 2010–2011; (b) N deposition and inputs under three typical meteorological years ( $P_r = 10\%$ ,  $50\%$ ,  $90\%$ ) and predicted for the years 2015 and 2020; (c) temporal variation of proportions attributable to N depositions; and (d) proportions under three typical meteorological years and predicted for the years 2015 and 2020. Note: The N input estimation and uncertainty are shown as a mean value (curve) and SD (shaded area) derived from the LOADEST; N deposition is shown as a mean value (curve) and 1-sigma (shaded area) derived from the Monte Carlo simulation; all error bars for fluxes or inputs are one SD; N deposition and inputs and the predicted proportions in 2015 and 2020 were calculated based on the methodology in Text S3.

wet deposition ( $24.3 \pm 7.5 \text{ mg km}^{-2} \text{ s}^{-1}$ , 52.2%), followed by ON ( $11.9 \pm 5.4 \text{ mg km}^{-2} \text{ s}^{-1}$ , 25.6%) and  $\text{NH}_4^+\text{-N}$  ( $10.3 \pm 3.9 \text{ mg km}^{-2} \text{ s}^{-1}$ , 22.2%). The corresponding concentrations of diverse N species at all 5 sites can be found in Figure S1. Peak N fluxes of wet deposition occurred in the wet season (i.e., from later July to

early October; Figure 2d), following the dry deposition peaks. The N flux during this period were up to  $172.9 \pm 72.2 \text{ mg km}^{-2} \text{ s}^{-1}$ , 6-fold greater than mean value of the rest of the year. N fluxes from January to March were only  $4.4 \pm 7.7 \text{ mg km}^{-2} \text{ s}^{-1}$ , due to this being the period of lowest precipitation (Figure 2d). This

trend of wet deposition fluxes was highly consistent with precipitation patterns over all 5 sites ( $r = 0.83$ ,  $P < 0.001$ ; Figure S3), but it was not significantly correlated with N concentrations ( $r = 0.32$ ,  $P < 0.001$ ; Figure S3). Seasonal changes of  $\text{NO}_3^-$ -N and ON were analogous to the total flux of wet deposition, whereas the changes of  $\text{NH}_4^+$ -N matched up best with dry deposition.

In addition, Figure S4 showed that the ratio of dry to wet deposition of N was 0.91 for the entire period but increased by more than 1.40 in early spring and winter. The ratio of reduced N ( $\text{NH}_3 + \text{NH}_4^+$ -N) to oxidized N ( $\text{NO}_2 + \text{NO}_3^-$ -N +  $\text{HNO}_2/\text{HNO}_3$ ) in total (wet plus dry) N deposition fluxes was more than 1.4 (Figure S4). The ratio increased to 1.7–3.8 in May, early July, and later August (Figure S4). This was slightly larger than national averages<sup>12</sup> (1.2), but smaller than ratios reported for the United States<sup>15</sup> (1.3–3.5).

**Riverine N Inputs.** Using the observed daily discharge as an independent variable, the LOADEST was able to reproduce observed N inputs from watersheds to Waihai, as shown by a coefficient of determination ( $R^2$ ) of 0.89 and the AIC of 1.8 (Figure 3). In the case of riverine N inputs to Caohai,  $R^2$  and AIC were 0.94 and 1.4 (Figure 3), respectively. Thus, the biweekly observations of N inputs from rivers estimated by the LOADEST could be converted into daily values. A Monte Carlo ensemble simulation<sup>38</sup> was performed to estimate the uncertainty of the riverine N inputs in this study. The calibrated LOADEST equations in Table S2 were run 100 000 times by randomly varying all of the model coefficients given a normal distribution given by the coefficients of variation (CVs), where uniform distribution was applied for streamflow. The CV of each model coefficient is estimated in the calibration process of LOADEST, and the CV of streamflow is assumed as 0.05. The mean value for N inputs from watersheds (including diffusive discharge from small creek rather than 19 rivers in Figure 1) to Lake Dianchi was  $12.5 \pm 12.2 \text{ t day}^{-1}$  ( $1\sigma$  as the standard deviation of N inputs occurring in 365 days; Figure 3), with  $8.5 \pm 7.9 \text{ t day}^{-1}$  for the Waihai and  $4.1 \pm 5.3 \text{ t day}^{-1}$  for the Caihai segments. Similarly, daily riverine inputs of different N constituents were estimated by means of LOADEST. Figure S5 showed that organic N comprised 45% of the total riverine inputs for the Waihai portion during the period 2010–2011, while  $\text{NH}_4^+$ -N contributed 57% for the Caohai portion. In addition, riverine inputs of  $\text{NO}_3^-$ -N accounted for 20% and 6% for the Waihai and Caohai portions, respectively.

**Contributions from Atmospheric Deposition.** Combining dry and wet deposition with daily riverine inputs of N, we derived the mean proportion of atmospheric N deposition to total N loads (i.e., sum of atmospheric deposition and riverine inputs), which was  $16.0 \pm 0.8\%$  for the period 2010–2011, during an extremely dry period with precipitation of  $707 \text{ mm yr}^{-1}$  (Figure 4a). The standard deviation due to uncertainties from deposition velocities (assuming  $\text{CV} = 10\%$ ), sampling processes (assuming  $\text{CV} = 5\%$ ), and riverine N inputs was determined by a Monte Carlo ensemble simulation.<sup>38</sup> More importantly, the contribution made by atmospheric N deposition increased to  $27 \pm 5$ – $48 \pm 8\%$  of total N loads in later spring and early summer (Figure 4c). To validate the robustness of our result, we further predicted the contributions of atmospheric N deposition under different precipitation scenarios according to Pearson Type III distribution (1956–2011).<sup>39</sup> Figure S6 demonstrated that precipitation at 10<sup>th</sup>, 50<sup>th</sup>, and 90<sup>th</sup> percentiles ( $P_t$ ) of the Pearson Type III distribution were 1305.3, 974.4, and 741.5  $\text{mm yr}^{-1}$ , respectively. Both river discharges and fluxes of wet

deposition were then linearly converted accordingly, where riverine N inputs were estimated using eq 1. N form and dry deposition flux were simply assumed equivalent to be the level in the period 2010–2011. Unexpectedly, the mean proportions of atmospheric N deposition to total N loads remained in a range from 15.7% to 16.6% during changing precipitation conditions.

The contribution from atmospheric N deposition to Lake Dianchi was further predicted under different reduction of riverine N inputs in recent year and into the future (Figure 4d). Details of the methodology can be found in Text S3. Indeed, recent observations in 2015 (Table S3) and the 13th Watershed Plan for Lake Dianchi ([http://xw.kunming.cn/a/2016-09/01/content\\_4349367.htm](http://xw.kunming.cn/a/2016-09/01/content_4349367.htm)) indicate that riverine N inputs decrease to  $3,146 \pm 342 \text{ t N yr}^{-1}$  in 2015 and  $2,608 \pm 226 \text{ t N yr}^{-1}$  in 2020, 31.1% and 42.9% lower than during 2010–2011 (Figure 4b and Table S3), respectively. This is mainly due to more rigorous controls on domestic sewage and urban stormwater discharge into Lake Dianchi.<sup>21</sup> If we assume that there will be no substantial improvement of air quality in the near future, then the proportion of atmospheric N deposition to total N loads into Lake Dianchi increases to 25.5% (2015) and 29.2% (2020) accordingly (Figure 4d).

## DISCUSSION

Reliable estimation of the contributions made by atmospheric N deposition is fundamental to our understanding of the lake N budget and is needed to enable policy makers to formulate a comprehensive N management plan.<sup>13</sup> However, previous estimates of the proportion of atmospheric N deposition to total N loads showed large discrepancies using traditional approaches.<sup>9,11</sup> This is mainly due to the lack of consideration of diverse N forms in atmospheric deposition and lack of direct observations of riverine inputs. Our high-resolution observations of N deposition, along with simultaneous measurements of riverine N inputs, permit new insight into the contribution of N deposition for a typical eutrophic lake.

Recently, gaseous and particulate inorganic N have been measured systematically in the Nationwide Nitrogen Deposition Monitoring Network (NNDMN) in China,<sup>12</sup> conducted by China Agricultural University. Two of 43 sites over vegetation were located close to Lake Dianchi and were operated from April 2009 to March 2010. Mean concentrations of  $\text{NH}_3$ ,  $\text{HNO}_2/\text{HNO}_3$ , and  $\text{NO}_2$  at the two sites of NNDMN ( $7.0$ ,  $6.3$ , and  $0.75 \mu\text{g N m}^{-3}$ ) were consistent with those of our study ( $7.6$ ,  $6.5$ , and  $0.98 \mu\text{g N m}^{-3}$ ), but slightly larger in particulate N ( $1.44$  v.s.  $1.10 \mu\text{g N m}^{-3}$ ; Figure S1). Accordingly, dry deposition of gaseous N and particulate inorganic N in our study ( $10.5 \pm 0.3$  and  $0.67 \pm 0.1 \text{ kg N ha}^{-1} \text{ yr}^{-1}$ ) were 44.7% and 46.0% lower than the mean values of the two sites in NNDMN ( $19.0 \pm 0.7$  and  $1.2 \pm 0.6 \text{ kg N ha}^{-1} \text{ yr}^{-1}$ ), respectively. Such a large discrepancy is primarily due to the difference in deposition velocities of  $\text{NO}_2$  and  $\text{HNO}_2/\text{HNO}_3$  (Figure S2) and additionally due to the difference in concentration of particulate N (Figure S1). For example, due to a larger surface resistance ( $R_c$ ) over water compared to land use types,<sup>40</sup> the mean value of  $V_d$  for  $\text{NO}_2$  in our study ( $0.0049 \pm 0.00009 \text{ m s}^{-1}$ ) was much lower than that over vegetation<sup>12</sup> ( $0.18 \pm 0.08 \text{ m s}^{-1}$ ) but close to that over oceanic water<sup>33</sup> ( $0.0053 \pm 0.003 \text{ m s}^{-1}$ ).  $V_d$  for  $\text{HNO}_2/\text{HNO}_3$  over Lake Dianchi ( $0.39 \pm 0.27 \text{ m s}^{-1}$ ) was only one-quarter of that over vegetation but approximately two-thirds of that over the coastal ocean<sup>12</sup> (Figure S2). Indeed,  $\text{HNO}_2/\text{HNO}_3$  is prone to dissolve in water and its  $R_c$  can be negligible,<sup>34</sup> the lower  $V_d$  for  $\text{HNO}_2/\text{HNO}_3$  over water may be therefore due to the changing aerodynamic

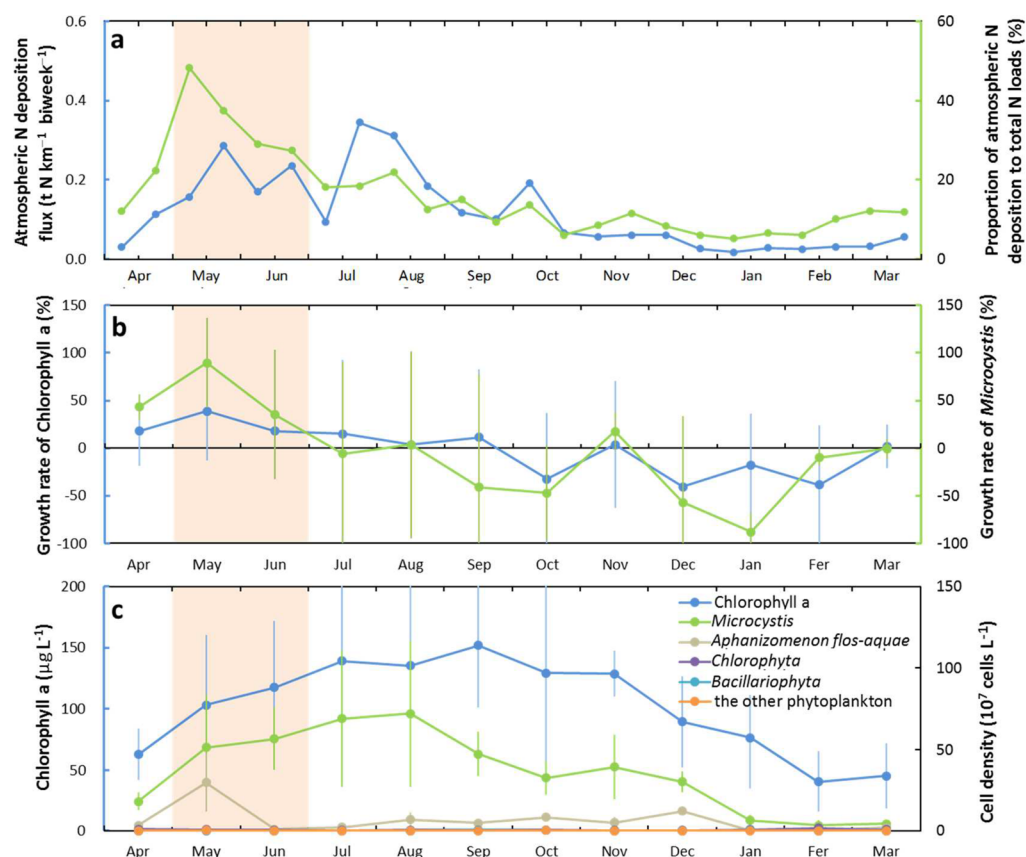


**Figure 5.** Temporal trends of N deposition and phytoplankton abundance. (a) N deposition fluxes and proportion of N deposition to total N loads; (b) mean monthly Chlorophyll *a* and cell density of diverse phytoplankton; (c) mean monthly growth rate for diverse phytoplankton. Details of observations can be found in the supporting references.<sup>47</sup> Phytoplankton population includes *Microcystis* spp., *Aphanizomenon flos-aquae*, Chlorophyta, Bacillariophyta, and the others; Growth rate is defined as the proportional change rate of Chlorophyll *a* and cell density  $X(t)$  as  $r(X) = X^{-1}dX/dt$ , where  $t$  is time step (i.e., monthly); Error bar indicated one standard deviation that represents interannual variability; Shaded area represents the critical period of late spring and early summer.

resistance along the gradient of wind speed or roughness length.<sup>30</sup> Lake Dianchi has a smaller roughness length compared to vegetation surface, meaning it has higher aerodynamic resistance. Relative to oceanic water, wind speed over Lake Dianchi is indeed lower and thus results in a smaller  $V_d$  for  $\text{HNO}_2/\text{HNO}_3$ . In addition, annual mean fluxes of  $\text{NH}_3$  over Lake Dianchi were greater than the national averages over the surface rather than waters ( $26.0 \text{ mg km}^{-2} \text{ s}^{-1}$ )<sup>12</sup> and mean values across United States<sup>15</sup> and European countries,<sup>14</sup> but less for the rest forms of dry deposition of N.

Our results also indicate that  $\text{NH}_3$  dominated the fluxes of dry deposition over Lake Dianchi. The seasonality of  $\text{NH}_3$  deposition, consistent with previous observations,<sup>12</sup> was not surprising. First, a growing number of field experiments indicate that  $\text{NH}_3$  volatilization from croplands increases with air temperature in a nonlinear manner.<sup>41</sup> This temperature-dependent relationship implies that  $\text{NH}_3$  deposition flux remained higher in warm season than cool season, even though  $V_d$  over Lake Dianchi is relatively lower in summer and autumn (Figure S2). To further understand the peaks of  $\text{NH}_3$  deposition flux, in-house surveys of farmers were conducted in the Lake Dianchi watershed. Three hundred representative farmers were selected for a face-to-face questionnaire-based household survey to collect information on fertilizer use in 13 towns surrounding Lake Dianchi (Figure S7). Figure S7 showed that high rates of N fertilizer use mainly occur in April, June, and July ( $367.7$ ,  $473.4$ ,  $568.7 \text{ kg N ha}^{-1} \text{ month}^{-1}$ , respectively), partly explaining the

large amount of  $\text{NH}_3$  volatilization<sup>42</sup> and hence abrupt increase of local deposition over the lake ( $<1 \text{ km}$ )<sup>43</sup> from late May onward. In contrast, the fluxes of N oxidation products decreased in summer compared to those in other seasons at 5 sites, in agreement with previous observations in South China.<sup>44</sup> Such seasonal patterns could be explained by discrepancies in atmospheric mixing and photochemical reactions between cold and warm seasons.<sup>44</sup>

Likewise, wet or bulk deposition of  $\text{NH}_4^+-\text{N}$  and  $\text{NO}_3^--\text{N}$  has been measured systematically in China.<sup>12</sup> Inorganic N is therefore used in the following comparative analysis. Wet deposition of inorganic N in this study ( $10.9 \text{ kg N ha}^{-1} \text{ yr}^{-1}$ ) was larger than the precipitation-adjusted annual mean flux ( $7.7 \text{ kg N ha}^{-1} \text{ yr}^{-1}$ ,  $n = 2$ ) at the two NNDMN sites,<sup>12</sup> but approximately one-third less than observation-based “diagnostic” value from bulk N deposition ( $14.5 \text{ kg N ha}^{-1} \text{ yr}^{-1}$  adjusted according to precipitation difference between 2000s and 2010–2011 in Lake Dianchi).<sup>12</sup> These discrepancies between our current and previous estimates stem from both site-to-site variation and sampling method differences. In our study, wet deposition of inorganic N in KM and JN was comparable to that of the two sites in NMDMN but 25% less than that in the other 3 sites (BF, CG, HK) located in east and west portions of Lake Dianchi. Thus, the mean wet deposition of the 5 sites exceeded that of the two sites in NMDMN. In addition, bulk N deposition used in previous observations denotes the deposition flux as a combination of wet deposition and partial dry deposition (e.g.,

coarse particle). Comparative experimental studies showed that the proportion of dry deposition accounts for approximately 25% of bulk N deposition.<sup>45</sup> When excluding the fraction attributable to dry deposition, observation-based “diagnostic” N deposition was decreased to 10.8 kg N ha<sup>-1</sup> yr<sup>-1</sup>, almost equal to our estimate of wet N deposition.

In addition to atmospheric deposition, the reliability of riverine N inputs strongly influences estimates of the relative contribution made by atmospheric N deposition. Fortunately, the state-of-the-art LOADEST has proven to be an effective tool to estimate daily loads from biweekly sampling, based on the empirical relationship with daily discharges. However, when using monthly concentrations and discharges from the routine monitoring program of local government (i.e., green solid circles in Figure 3), total N inputs from all rivers were changed to 5589 t N yr<sup>-1</sup>, which was 22.4% greater than our observations. Consequently, the contribution made by N deposition decreased to 13% of the total N load. Ambient NH<sub>3</sub> has not been historically and routinely measured due to lack of specific regulatory requirements for its measurement. If we further exclude the dry deposition of NH<sub>3</sub>, then the proportion of N deposition to total N loads declined to 8.9%, which is comparable to previous estimates (7.6%).<sup>46</sup> This new finding suggests that the importance of atmospheric N deposition has likely been underestimated, especially for eutrophic lakes close to intensively managed farmland.

Our scenario-based predictions indicated that atmospheric N deposition is a quantitatively important source of biologically available N input in Lake Dianchi (Figure 4d). Furthermore, the role in atmospherically deposited N may increase if no effective controls on emissions are undertaken (Figure 4d). With regard to the lake’s cyanobacterial (e.g., *Microcystis*) bloom formation and proliferation, the relative contribution to total external N loading was highest (27 ± 5–48 ± 8% of total N loads) in late spring and early summer (Figure 4c). This period coincides with that of maximum phytoplankton growth (measured as chlorophyll-a in the period of 2009–2012, 18–39% month<sup>-1</sup>; Figure 5b), and can in part support phytoplankton production, leading to maximal biomass accumulation in early autumn (152 μg L<sup>-1</sup>; Figure 5c). Specifically, for the cyanobacterial bloom former *Microcystis* spp. which accounts for 84% of phytoplankton abundance,<sup>47</sup> an initial spring proliferation (51.4 × 10<sup>7</sup> to ~6.7 × 10<sup>7</sup> cell L<sup>-1</sup>; Figure 5c) and maximum growth rate (35–90% month<sup>-1</sup>; Figure 5b) overlap closely with the period of maximum atmospheric N deposition relative to total N inputs (Figure 5a). In addition, during the summer *Microcystis* blooms in Lake Dianchi, soluble reactive phosphorus (SRP) concentrations remained quite high in the water column, while dissolved inorganic N decreased rapidly (Figure S8). N availability therefore controlled biomass production if having excess SRP in the lake.<sup>48,50</sup> A similar scenario has been observed in eutrophic Lake Taihu, China, which like Lake Dianchi is impacted by summer *Microcystis* blooms. In situ nutrient enrichment bioassays have shown these blooms to be largely N-limited.<sup>48,50</sup> This temporal linkage implies that atmospheric N deposition, as a highly significant N source, may support *Microcystis* growth during the critical initial proliferation period and for sustaining summer blooms in Lake Dianchi. It should be noted that this toxic bloom-forming genus is not a nitrogen (N<sub>2</sub>) fixer and hence has a strong requirement for externally supplied N to support growth.<sup>48–50</sup> This places even more weight on timely and quantitatively significant inputs of atmospheric N deposition during a period of maximum bloom potential and N

demand by this genus. To confirm this scenario, in situ bioassays should be conducted in the future to determine seasonal patterns of N limitation and thresholds for cyanobacteria growth.<sup>48</sup> To mitigate the heavily N-dependent *Microcystis* growth during this critical period, N emissions that dominates the flux of N deposition into Lake Dianchi should be effectively controlled in addition to the reduction of riverine N inputs. For example, cropland NH<sub>3</sub> volatilization in the watershed can be reduced through site-specific nitrogen management<sup>51</sup> that aims to optimize the supply of fertilizers over time and space while maintaining or enhancing crop yields.

At present, the contribution made by atmospheric N deposition to the total N inputs contains some uncertainties and is influenced by factors related to data sets used in calculation and scope of sampling.  $V_d$  of gaseous N over the water were calculated using deposition velocity model based on local meteorological data, which was not validated by direct observations. Chemical form of gaseous and particulate N also depends on meteorological conditions and atmospheric composition (e.g., humidity, temperature, oxygen radicals). Any change in these factors will result in differences in atmospheric N deposition over lake surface. In addition, runoff of atmospheric N deposition from watersheds (i.e., indirect deposition) to Lake Dianchi, was not measured or estimated in this study. However, NO<sub>3</sub><sup>-</sup>-N, a highly soluble N in water,<sup>52,53</sup> was a dominant N constituent in precipitation (Figure 2c). If assuming no differences in NO<sub>3</sub><sup>-</sup>-N concentrations in precipitation between the sites around and away from the lake, then N deposition flowing into the lake from watershed runoff was at least 141.1 t N during 2010–2011, which was calculated as the product of mean NO<sub>3</sub><sup>-</sup>-N concentration in wet samples from 5 monitoring sites and the portion of streamflow generated from the excess rainfall during a major storm event (see details in Text S4 and Figure S9). Accordingly, the contribution of annual N deposition to total N loads increased from 16% (direct portion) to >18% (direct and indirect portions). Therefore, further efforts at making long-term measurements of dry deposition using relaxed eddy accumulation systems<sup>17</sup> are needed. In addition, the contribution of indirect N deposition on watersheds needs to be determined. Lastly, groundwater discharge, as an additional N input to the lake, was also not included because no measurements were available. We estimated it using a lake water balance approach for the period of April 2010 - March 2011 (see details in Text S5). Figure S10 indicated that groundwater discharge (3.6 × 10<sup>6</sup> m<sup>3</sup> yr<sup>-1</sup>) was much lower than streamflow during study period (380.9 × 10<sup>6</sup> m<sup>3</sup> yr<sup>-1</sup>). Although uncertainties exist in this estimate, N contributions from groundwater discharge were considered negligible.

In summary, atmospheric N deposition proved to be an important source of N to Lake Dianchi, especially during initial proliferation and periods of maximum *Microcystis* bloom formation. Decreases in riverine N inputs from watersheds are expected to continue into the future as China aims to lower the N inputs from reuse of reclaimed water and urban stormwater.<sup>54</sup> Current projections of increasing NH<sub>3</sub> emissions,<sup>55</sup> meanwhile, suggest that N deposition levels, especially reduced N, will increase and form a larger fraction of total N loading to the lake in the future. We note that reduced N (as NH<sub>4</sub><sup>+</sup>) is the preferred N source for bloom-forming cyanobacteria, including *Microcystis* spp.<sup>49</sup> Compared to Lake Dianchi, the contribution made by atmospheric N depositions may be even greater in other eutrophic lakes in East and North China which are experiencing extremely poor air quality.<sup>12</sup> Although China’s Central Govern-



ment has issued regulatory policies for cleaner air and water,<sup>54,56</sup> local administrators still face challenges in coordinating the reductions of atmospheric deposition and riverine inputs, given limited financial resources. In addition to implementing a comprehensive assessment of watershed N loads (i.e., N deposition and inputs) in China, identifying effective approaches that yield positive benefits for both air and water quality remains a high priority for lake ecosystem management.

## ■ ASSOCIATED CONTENT

### ● Supporting Information

The Supporting Information is available free of charge on the ACS Publications website at DOI: [10.1021/acs.est.6b06135](https://doi.org/10.1021/acs.est.6b06135).

Details of sampling design, deposition velocity models, details of atmospheric depositions at 5 sites, results of in-house surveys, and the other information (PDF)

## ■ AUTHOR INFORMATION

### Corresponding Author

\*Phone: +86 10 62756511; fax: +86 10 62756560; e-mail: [zhouf@pku.edu.cn](mailto:zhouf@pku.edu.cn) (F.Z.).

### ORCID

Feng Zhou: 0000-0001-6122-0611

Shu Tao: 0000-0002-7374-7063

### Author Contributions

▲X.Y.Z. and Y.B. contributed equally to this work.

### Notes

The authors declare no competing financial interest.

## ■ ACKNOWLEDGMENTS

This study was supported by the National Key Research and Development Program of China (2016YFD0800501), the National Natural Science Foundation of China (41671464, 41425007, and 41371303), and 111 Project (B14001). H.P. was supported by the U.S. National Science Foundation Dimensions of Biodiversity project 1240851 and by the Chinese Ministry of Science and Technology (MOST), contract 2014zx07101-011. We appreciated KEMC and Prof. Yonghua Wang (Peking University) for collecting and analyzing samples. We also appreciated Prof. Lirong Song (Chinese Academy of Sciences) for providing data of lake N, P, and phytoplankton.

## ■ REFERENCES

- (1) Duce, R. A.; LaRoche, J.; Altieri, K.; Arrigo, K. R.; Baker, A. R.; Capone, D. G.; Cornell, S.; Dentener, F.; Galloway, J.; Ganeshram, R. S.; Geider, R. J.; Jickells, T.; Kuypers, M. M.; Langlois, R.; Liss, P. S.; Liu, S. M.; Middelburg, J. J.; Moore, C. M.; Nickovic, S.; Oschlies, A.; Pedersen, T.; Prospero, J.; Schlitzer, R.; Seitzinger, S.; Sorensen, L. L.; Uematsu, M.; Ulloa, O.; Voss, M.; Ward, B.; Zamora, L. Impacts of atmospheric anthropogenic nitrogen on the open ocean. *Science* **2008**, *320* (5878), 893–897.
- (2) Peñuelas, J.; Poulter, B.; Sardans, J.; Ciais, P.; van der Velde, M.; Bopp, L.; Boucher, O.; Godderis, Y.; Hinsinger, P.; Llusia, J.; Nardin, E.; Vicca, S.; Obersteiner, M.; Janssens, I. A. Human-induced nitrogen-phosphorus imbalances alter natural and managed ecosystems across the globe. *Nat. Commun.* **2013**, *4* (1), 94–105.
- (3) Wang, R.; Balkanski, Y.; Bopp, L.; Aumont, O.; Boucher, O.; Ciais, P.; Gehlen, M.; Peñuelas, J.; Ethé, C.; Hauglustaine, D. Influence of anthropogenic aerosol deposition on the relationship between oceanic productivity and warming. *Geophys. Res. Lett.* **2015**, *42* (24), 10745–10754.
- (4) Elser, J. J.; Andersen, T.; Baron, J. S.; Bergström, A. K.; Jansson, M.; Kyle, M.; Nydick, K. R.; Steger, L.; Hessen, D. O. Shifts in lake N:P

stoichiometry and nutrient limitation driven by atmospheric nitrogen deposition. *Science* **2009**, *326* (5954), 835–837.

- (5) Paerl, H. W. Enhancement of marine primary production by nitrogen-enriched acid rain. *Nature* **1985**, *315* (6022), 747–749.

- (6) Paerl, H. W. Coastal eutrophication and harmful algal blooms: Importance of atmospheric deposition and groundwater as “new” nitrogen and other nutrient sources. *Limnol. Oceanogr.* **1997**, *42* (5), 1154–1165.

- (7) Bergström, A. K.; Jansson, M. Atmospheric nitrogen deposition has caused nitrogen enrichment and eutrophication of lakes in the northern hemisphere. *Global Chang. Biol.* **2006**, *12* (4), 635–643.

- (8) Liu, X. J.; Duan, L.; Mo, J. M.; Du, E. Z.; Shen, J. L.; Lu, X. K.; Zhang, Y.; Zhou, X. B.; He, C. E.; Zhang, F. S. Nitrogen deposition and its ecological impact in China: An overview. *Environ. Pollut.* **2011**, *159* (10), 2251–2264.

- (9) Luo, L. C.; Qin, B. Q.; Yang, L. Y.; Song, Y. Z. Total inputs of phosphorus and nitrogen by wet deposition into Lake Taihu, China. *Hydrobiologia* **2007**, *194* (1), 63–70.

- (10) Yan, Z.; Han, W.; Penuelas, J.; Sardans, J.; Elser, J. J.; Du, E.; Reich, P. B.; Fang, J. Phosphorus accumulates faster than nitrogen globally in freshwater ecosystems under anthropogenic impacts. *Ecol. Lett.* **2016**, *19* (10), 1237–1246.

- (11) Morales, J. A.; Albornoz, A.; Socorro, E.; Morillo, A. An estimation of the nitrogen and phosphorus loading by wet deposition over Lake Maracaibo, Venezuela. *Water, Air, Soil Pollut.* **2001**, *128* (3), 207–221.

- (12) Xu, W.; Luo, X. S.; Pan, Y. P.; Zhang, L.; Tang, A. H.; Shen, J. L.; Zhang, Y.; Li, K. H.; Wu, Q. H.; Yang, D. W.; Zhang, Y. Y.; Xue, J.; Li, W. Q.; Li, Q. Q.; Tang, L.; Lu, S. H.; Liang, T.; Tong, Y. A.; Liu, P.; Zhang, Q.; Xiong, Z. Q.; Shi, X. J.; Wu, L. H.; Shi, W. Q.; Tian, K.; Zhong, X. H.; Shi, K.; Tang, Q. Y.; Zhang, L. J.; Huang, J. L.; He, C. E.; Kuang, F. H.; Zhu, B.; Liu, H.; Jin, X.; Xin, Y. J.; Shi, X. K.; Du, E. Z.; Dore, A. J.; Tang, S.; Collett, J. L., Jr.; Goulding, K.; Sun, Y. X.; Ren, J.; Zhang, F. S.; Liu, X. J. Quantifying atmospheric nitrogen deposition through a nationwide monitoring network across China. *Atmos. Chem. Phys.* **2015**, *15*, 12345–12360.

- (13) Castro, M. S.; Driscoll, C. T. Atmospheric nitrogen deposition to estuaries in the mid-Atlantic and northeastern United States. *Environ. Sci. Technol.* **2002**, *36* (15), 3242–3249.

- (14) EANET. *The Second Periodic Report on the State of Acid Deposition in East Asia*; 2000.

- (15) Li, Y.; Schichtel, B. A.; Walker, J. T.; Schwede, D. B.; Chen, X.; Lehmann, C. M.; Puchalski, M. A.; Gay, D. A.; Collett, J. L. Increasing importance of deposition of reduced nitrogen in the United States. *Proc. Natl. Acad. Sci. U. S. A.* **2016**, *113* (21), 5874–5879.

- (16) EMEP. *Data Report, Acidifying and Eutrophying Compounds*, 2014.

- (17) Myles, L.; Meyers, T. P.; Robinson, L. Relaxed eddy accumulation measurements of ammonia, nitric acid, sulfur dioxide and particulate sulfate dry deposition near Tampa, FL, USA. *Environ. Res. Lett.* **2007**, *2* (3), 241–285.

- (18) Dolislager, L. J.; VanCuren, R.; Pederson, J. R.; Lashgari, A.; McCauley, E. A summary of the Lake Tahoe Atmospheric Deposition Study (LTADS). *Atmos. Environ.* **2012**, *46*, 618–630.

- (19) He, B.; Wang, Y.; Razafindrabe, B. H. N.; Abe, M.; Oki, T. Analysis of long term nitrogen loads from point and diffuse pollutant sources in Lake Biwa, Japan. [http://wldb.ilec.or.jp/data/ilec/WLC13\\_Papers/others/S2.pdf](http://wldb.ilec.or.jp/data/ilec/WLC13_Papers/others/S2.pdf).

- (20) Seitzinger, S. P.; Harrison, J. A.; Dumont, E.; Beusen, A. H. W.; Bouwman, A. F. Sources and delivery of carbon, nitrogen, and phosphorus to the coastal zone: An overview of Global Nutrient Export from Watersheds (NEWS) models and their application. *Global Biogeochem. Cycles* **2005**, *19* (4), 1064–1067.

- (21) Zhang, X. L.; Zou, R.; Wang, Y. L.; Liu, Y.; Zhao, L.; Zhu, X.; Guo, H. C. Is water age a reliable indicator for evaluating water quality effectiveness of water diversion projects in Eutrophic lakes? *J. Hydrol.* **2016**, *542*, 281–291.

- (22) Yang, Y. H.; Zhou, F.; Guo, H. C.; Sheng, H.; Liu, H.; Dao, X.; He, C. J. Analysis of spatial and temporal water pollution patterns in Lake Dianchi using multivariate statistical methods. *Environ. Monit. Assess.* **2010**, *170* (1–4), 407–416.

- (23) Sather, M. E.; Slonecker, E. T.; Mathew, J.; Daughtrey, H.; Williams, D. D. Evaluation of Ogawa passive sampling devices as an alternative measurement method for the nitrogen dioxide annual standard in El Paso, Texas. *Environ. Monit. Assess.* **2007**, *124* (1–3), 211–221.
- (24) Jovan, S.; Riddell, J.; Padgett, P. E.; Nash, T. H. Eutrophic lichens respond to multiple forms of N: implications for critical levels and critical loads research. *Ecol. Appl.* **2012**, *22* (7), 1910–1922.
- (25) Roadman, M. J.; Scudlark, J. R.; Meisinger, J. J.; Ullman, W. J. Validation of Ogawa passive samplers for the determination of gaseous ammonia concentrations in agricultural settings. *Atmos. Environ.* **2003**, *37* (17), 2317–2325.
- (26) Bytnerowicz, A.; Sanz, M. J.; Arbaugh, M. J.; Padgett, P. E.; Jones, D. P.; Davila, A. Passive sampler for monitoring ambient nitric acid (HNO<sub>3</sub>) and nitrous acid (HNO<sub>2</sub>) concentrations. *Atmos. Environ.* **2005**, *39* (39), 2655–2660.
- (27) Wang, Z.; Zou, R.; Zhu, X.; He, B.; Yuan, G.; Zhao, L.; Liu, Y. Predicting lake water quality responses to load reduction: a three-dimensional modeling approach for total maximum daily load. *Int. J. Environ. Sci. Technol.* **2014**, *11* (2), 423–436.
- (28) Buchanan, T. J.; Somers, W. P. *Discharge Measurements at Gaging Stations*; U.S. Geological Survey Techniques of Water-Resources Investigations, Book 3, Chapter A8, pp 65, 1969.
- (29) State Environmental Protection Administration. *Standard Methods for the Examination of Water and Wastewater (version 4)*; 2002.
- (30) Kuang, F. H.; Liu, X. J.; Zhu, B.; Shen, J. L.; Pan, Y. P.; Su, M. M.; Goulding, K. Wet and dry nitrogen deposition in the central Sichuan Basin of China. *Atmos. Environ.* **2016**, *143*, 39–50.
- (31) Gualtieri, G.; Secci, S. Comparing methods to calculate atmospheric stability-dependent wind speed profiles: A case study on coastal location. *Renewable Energy* **2011**, *36* (8), 2189–2204.
- (32) Wesely, M. L.; Hicks, B. B. Some factors that affect the deposition rates of sulfur dioxide and similar gases on vegetation. *J. Air Pollut. Control Assoc.* **1977**, *27* (11), 1110–1116.
- (33) Zhang, Y.; Yu, Q.; Ma, W. C.; Chen, L. M. Atmospheric deposition of inorganic nitrogen to the eastern China seas and its implications to marine biogeochemistry. *J. Geophys. Res.* **2010**, *115* (11), 3421–3423.
- (34) Wesely, M. L. Parameterization of surface resistances to gaseous dry deposition in regional-scale number models. *Atmos. Environ.* **1989**, *23* (6), 1293–1304.
- (35) Slinn, W. G. N. Prediction for particle deposition to vegetative canopies. *Atmos. Environ.* **1982**, *16* (7), 1785–1794.
- (36) Zhang, L. M.; Gong, S. L.; Padro, J.; Barrie, L. A size-segregated particle dry deposition scheme for an atmospheric aerosol module. *Atmos. Environ.* **2001**, *35* (3), 549–560.
- (37) Runkel, R. L.; Crawford, C. G.; Cohn, T. A. *Load Estimator (LOADEST)—A FORTRAN Program for Estimating Constituent Loads in Streams and Rivers*; U.S. Geological Survey Techniques and Methods book 4, chap. A5: 2004.
- (38) Zhou, F.; Shang, Z. Y.; Ciais, P.; Tao, S.; Piao, S. L.; Raymond, P.; He, C. F.; Li, B. G.; Wang, R.; Wang, X. H.; Peng, S. S.; Zeng, Z. Z.; Chen, H.; Ying, N.; Hou, X. K.; Xu, P. A new high-resolution N<sub>2</sub>O emission inventory for China in 2008. *Environ. Sci. Technol.* **2014**, *48* (15), 8538–8547.
- (39) Griffiths, V. W.; Stedinger, J. R. Log-Pearson Type 3 Distribution and Its Application in Flood Frequency Analysis. I: Distribution Characteristics. *J. Hydrol. Eng.* **2007**, *12* (5), 482–491.
- (40) Zhang, L.; Brook, J. R.; Vet, R. A revised parameterization for gaseous dry deposition in air-quality models. *Atmos. Chem. Phys.* **2003**, *3* (6), 2067–2082.
- (41) Sommer, S. G.; Schjoerring, J. K.; Denmead, O. T. Ammonia emission from mineral fertilizers and fertilized crops. *Adv. Agron.* **2004**, *82* (3), 557–622.
- (42) Zhou, F.; Ciais, P.; Hayashi, K.; Galloway, J.; Kim, D. G.; Yang, C. L.; Li, S. Y.; Liu, B.; Shang, Z. Y.; Gao, S. S. Re-estimating NH<sub>3</sub> emissions from Chinese cropland by a new nonlinear model. *Environ. Sci. Technol.* **2016**, *50* (2), 564–572.
- (43) Asman, W. A. H.; Sutton, M. A.; Schjørring, J. K. Ammonia: emission, atmospheric transport and deposition. *New Phytol.* **1998**, *139* (1), 27–48.
- (44) Yang, R.; Hayashi, K.; Zhu, B.; Li, F.; Yan, X. Atmospheric NH<sub>3</sub> and NO<sub>2</sub> concentration and nitrogen deposition in an agricultural catchment of Eastern China. *Sci. Total Environ.* **2010**, *408* (20), 4624–4632.
- (45) Nadim, F.; Trahiotis, M. M.; Stapcinskaite, S.; Perkins, C.; Carley, R. J.; Hoag, G. E.; Yang, X. Estimation of wet, dry and bulk deposition of atmospheric nitrogen in Connecticut. *J. Environ. Monit.* **2001**, *3* (6), 671–680.
- (46) Jin, X. C. *Lakes in China—Research of Their Environment*; China Ocean Press: Beijing, China, 1995.
- (47) Wu, Y. L.; Li, L.; Zheng, L. L.; Dai, G. Y.; Ma, H. Y.; Shan, K.; Wu, H.; Zhou, Q.; Song, L. Patterns of succession between bloom-forming cyanobacteria *Aphanizomenon flos-aquae* and *Microcystis* and related environmental factors in large, shallow Dianchi Lake, China. *Hydrobiologia* **2016**, *765* (1), 1–13.
- (48) Xu, H.; Paerl, H. W.; Qin, B. Q.; Zhu, G. W.; Gao, G. A. Nitrogen and phosphorus inputs control phytoplankton growth in eutrophic Lake Taihu, China. *Limnol. Oceanogr.* **2010**, *55* (1), 420–432.
- (49) Paerl, H. W.; Xu, H.; Hall, N. S.; Rossignol, K. L.; Joyner, A. R.; Zhu, G. W.; Qin, B. Q. Nutrient limitation dynamics examined on a multi-annual scale in Lake Taihu, China: implications for controlling eutrophication and harmful algal blooms. *J. Freshwater Ecol.* **2015**, *30* (1), 5–24.
- (50) Paerl, H. W.; Xu, H.; McCarthy, M. J.; Zhu, G. W.; Qin, B. Q.; Li, Y. P.; Gardner, W. S. Controlling harmful cyanobacterial blooms in a hyper-eutrophic lake (Lake Taihu, China): The need for a dual nutrient (N & P) management strategy. *Water Res.* **2011**, *45* (5), 1973–1983.
- (51) Richards, M. B.; Butterbach-Bahl, K.; Jat, M. L.; Lipinski, B.; Ortiz-Monasterio, I.; Sapkota, T. Site-Specific Nutrient Management: Implementation Guidance for Policymakers and Investors. Climate-Smart Agriculture Practice Brief. In *CGIAR Research Program on Climate Change, Agriculture and Food Security (CCAFS)*; Copenhagen: Denmark, **2015**; pp 1–10.
- (52) Erickson, A. J.; Gulliver, J. S.; Arnold, W. A.; Brekke, C.; Bredal, M. Abiotic capture of stormwater nitrates with granular activated carbon. *Environ. Eng. Sci.* **2016**, *33* (5), 354–363.
- (53) Jury, W. A.; Nielsen, D. R. *Chapter 5—Nitrate Transport and Leaching Mechanisms*. 1989.
- (54) *Water Pollution Control Action Plan*; The State Council of the People's Republic of China: Beijing, China, 2015.
- (55) Sutton, M. A.; Reis, S.; Riddick, S. N.; Dragosits, U.; Nemitz, E.; Theobald, M. R.; Tang, Y. S.; Braban, C. F.; Vieno, M.; Dore, A. J.; Mitchell, R. F.; Wanless, S.; Daunt, F.; Fowler, D.; Blackall, T. D.; Milford, C.; Flechard, C. R.; Loubet, B.; Massad, R.; Cellier, P.; Personne, E.; Coheur, P. F.; Clarisse, L.; Van Damme, M.; Ngadi, Y.; Clerbaux, C.; Skjoth, C. A.; Geels, C.; Hertel, O.; Kruit, R. J. W.; Pinder, R. W.; Bash, J. O.; Walker, J. T.; Simpson, D.; Horvath, L.; Misselbrook, T. H.; Bleeker, A.; Dentener, F.; de Vries, W. Towards a climate-dependent paradigm of ammonia emission and deposition. *Philos. Trans. R. Soc., B* **2013**, *368* (1621), 125–134.
- (56) Zhang, Q.; He, K.; Huo, H. Policy: Cleaning China's air. *Nature* **2012**, *484* (7393), 161–162.